SUPPORTING INFORMATION

Towards single-molecule *in situ* electrochemical SERS detection with disposable substrates

Daniel Martín-Yerga, Alejandro Pérez-Junquera, María Begoña González-García, David Hernández-Santos, Pablo Fanjul-Bolado*

DropSens S.L. Edificio CEEI, Parque Tecnológico de Asturias, 33428 Llanera, Asturias, Spain

* Corresponding author: pfanjul@dropsens.com

EXPERIMENTAL

Instrumentation and electrodes

In situ dynamic Raman spectroelectrochemistry was performed using a compact and integrated instrument, SPELEC RAMAN (DropSens), which contains a laser source of 785 nm. This instrument was connected to a bifurcated reflection probe (DRP-RAMANPROBE) and a specific cell for screen-printed electrodes (DRP-RAMANCELL). The diameter of the laser spot was about 200 µm. This probe allows to get an average signal of a large surface area, and minimizes the irreproducibility produced by hot spots or non-active regions. The instrument was controlled by DropView SPELEC software, which allows to perform simultaneous and real-time spectroelectrochemical experiments, with totally synchronized data acquisition.

Screen-printed silver electrodes (DRP-C013, DropSens) were used throughout the work. These devices consist of a flat ceramic card on which a three-electrode system comprising the electrochemical cell is screen-printed. The working silver electrode is circular with a diameter of 1.6 mm, and the device has also an auxiliary electrode made of carbon and a silver electrode which acts as a pseudoreference. All spectroelectrochemical measurements were performed at room temperature and using a solution of 50 µL

for Raman, respectively. The reported potentials are related to the silver screen-printed pseudoreference electrode.

A JEOL 6610LV scanning electron microscope (SEM) was used to characterize the working silver electrodes at various stages of the electrochemical activation. This instrument was employed to record the energy-dispersive X-ray (EDX) spectra.

Reagents and solutions

Potassium ferricyanide, potassium chloride, potassium nitrate, lithium perchlorate, Tris(2,2-bipyridyl)dichlororuthenium(II) hexahydrate. Ultrapure water obtained with a Millipore DirectQ purification system from Millipore was used throughout this work.

Raman spectroelectrochemical measurements

Raman spectroelectrochemical experiments were performed by applying a linear sweep voltammetry in a range of potentials depending on the electrolyte employed at a scan rate of 50 mV/s, a step potential of 2 mV and equilibration time of 1 s. The potential range was from +0.3 to -0.4 V for chloride electrolytes and +0.5 to -0.4 V for non-chloride electrolytes. Raman spectra were registered with an integration time of 2 s and a laser power of 258 mW. In order to study the detection of ultralow concentrations, a chronoamperometric detection was used applying a potential of 0 V for 28 s after a previous activation with +0.40 V for 3 s. In this case, the Raman integration time was increased to 8 s in order to increase the number of scattered photons detected and the probability to detect them. Laser power was about 45 mW.

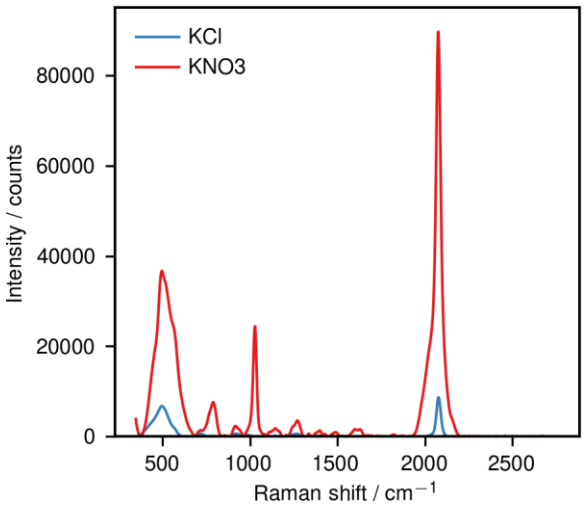

Figure S1. Spectra (baseline-corrected) obtained for 1x10^{-5} M ferricyanide after the substrate activation in KCl and KNO_3. Ferricyanide bands are observed in both experiments at 2076 and 495 cm^{-1}. Bands observed at 788 and 1028 cm^{-1} are due to nitrate vibrations, and they were not present in the KCl experiments. For the ferricyanide specific bands, the Raman shift of the peaks are similar in both experiments and the intensity increased for both peaks in KNO_3 at a similar extent. These facts suggest that the same kind of vibrations are involved in both experiments and the increment of the SERS signal is mainly due to the increased activity of the silver nanostructure. If the probe molecule interacts in a different orientation with the substrate, it would be expected some changes in the Raman shift or the intensity ratios between the two vibrational bands.

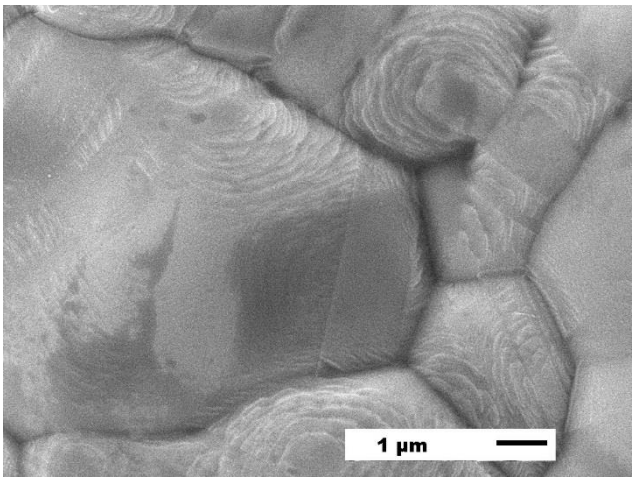

Figure S2. SEM image of the pristine surface of silver screen-printed electrode.

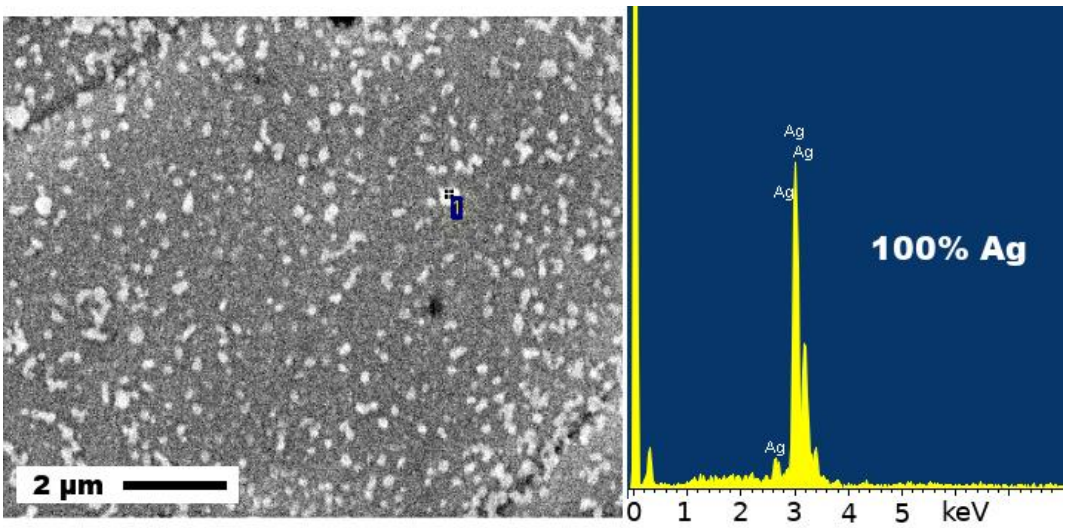

Figure S3. Representative SEM image of the silver screen-printed electrode after the *in situ* activation using KCl as electrolyte and EDX spectrum of one nanoparticle from the surface. This surface was obtained after the activation of the electrode from +0.3 V to -0.35 V, where the SERS signal was maximum. In this case, the voltammetric sweep was stopped when the AgCl generated initially has been reduced and elemental Ag is formed on the surface.

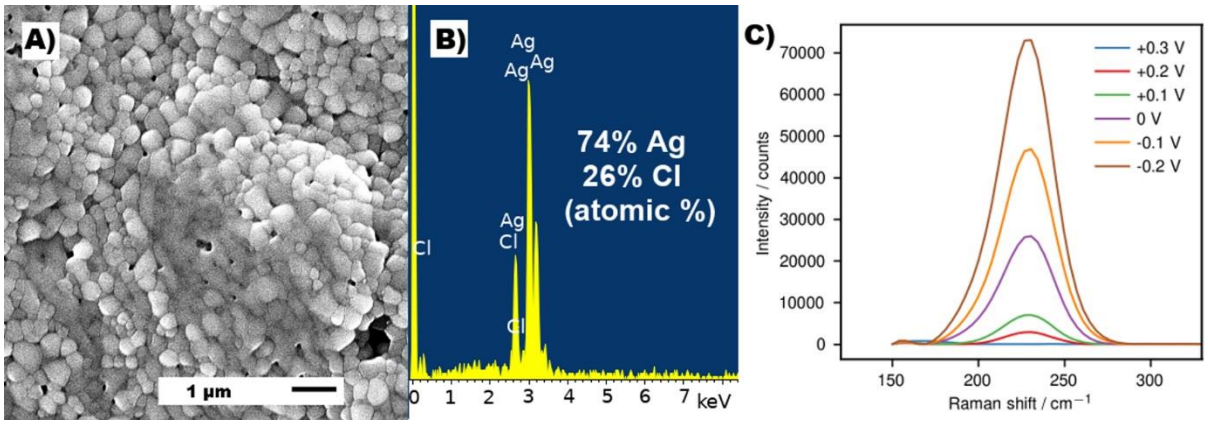

Figure S4. A) Representative SEM image of the silver screen-printed electrode after in situ activation from +0.3 V to +0.05 V using KCl as electrolyte and **B)** typical EDX spectrum of this surface. The electrochemical activation was stopped at potentials where only the oxidation of silver had occurred. The image shows a well-compacted surface composed of AgCl particles, which are generated after the oxidation of silver in presence of chloride ions. **C)** Raman spectra obtained between 150 and 300 cm^{-1} during the oxidation of the surface. The Raman band at 230 cm^{-1} increased during the oxidation step, confirming the generation of AgCl.

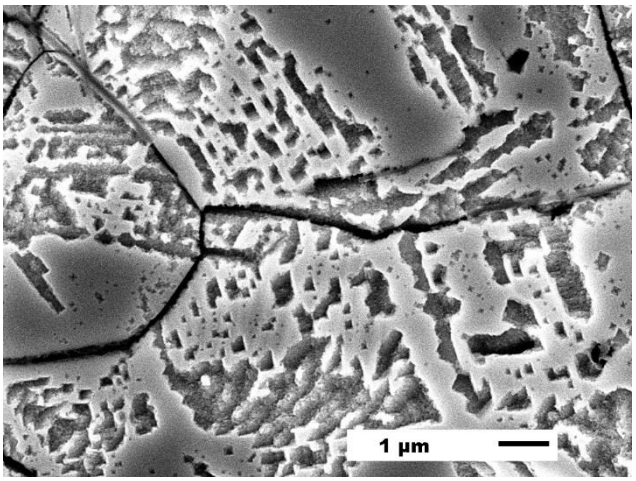

Figure S5. Representative SEM image of the silver screen-printed electrode after the *in situ* activation using KNO_3 as electrolyte. In this case, the voltammetric sweep was performed from +0.5 to +0.35 V (i.e. it was stopped during the oxidative stage). The initial silver electrode is oxidised resulting in an etched surface. This porous, rough surface seems to have a higher surface area than the initial pristine surface (see **Figure S2**), but this increment of the roughness did not increase the SERS signal. This fact suggests that this roughened silver is not SERS active and the increment of the surface area (visually observed) does not influence the SERS activity. The SERS signal only increased when fresh silver particles were generated during the reduction stage, demonstrating that the active surface area only comes from the new generated particles.

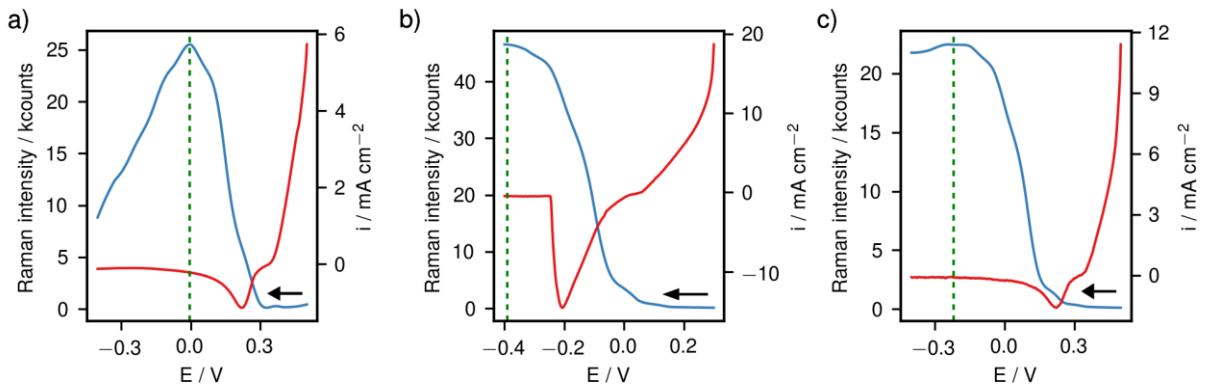

Figure S6. Evolution of the Raman peak intensity (baseline corrected) of different species (blue line) during the linear sweep voltammogram (red line) performed to activate the electrode surface with different electrolytes. Green lines show the potential for the maximum peak intensity. **A)** Peak intensity at 2076 cm^{-1} using a solution of $1x10^{-5}$ M $[Fe(CN)_6]^{3-}$ in 0.1 M $LiClO_4$. **B)** Peak intensity at 1036 cm^{-1} using a solution of $2x10^{-6}$ M $[Ru(bpy)_3]^{2+}$ in 0.1 M KCl. **C)** Peak intensity at 1036 cm^{-1} using a solution of $2x10^{-6}$ M $[Ru(bpy)_3]^{2+}$ in 0.1 M KNO_3.

The maximum peak intensity for $[Fe(CN)_6]^{3-}$ in 0.1 M $LiClO_4$ was c.a. 0 V. This case is similar to KNO_3 as the oxidation of silver does not form an insoluble product. This fact results in the reduction of soluble silver at more positive potentials than AgCl, and the maximum SERS effect after the generation of fresh silver is obtained c.a. 0 V. The SERS intensity in $LiClO_4$ was higher than that obtained in KCl, which seems to corroborate that the generation of fresh silver when the surface is charged more positively has a strong influence in the detection of anionic species such as $[Fe(CN)_6]^{3-}$ as observed for KNO_3 and KCl. In contrast, for cationic species such as $[Ru(bpy)_3]^{2+}$, the maximum SERS signal in a KCl electrolyte is obtained at about -0.4 V (30 mV more negative than $[Fe(CN)_6]^{3-}$). In KNO_3, the highest SERS signal was obtained at -0.20 V (about 200 mV more negative than $[Fe(CN)_6]^{3-}$), which corroborates that both the generation of fresh silver and the potential where the silver is generated influence the SERS signal of cationic and anionic species.

A) 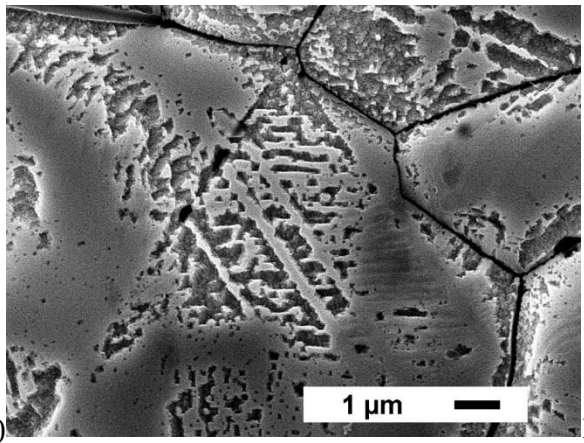

B) 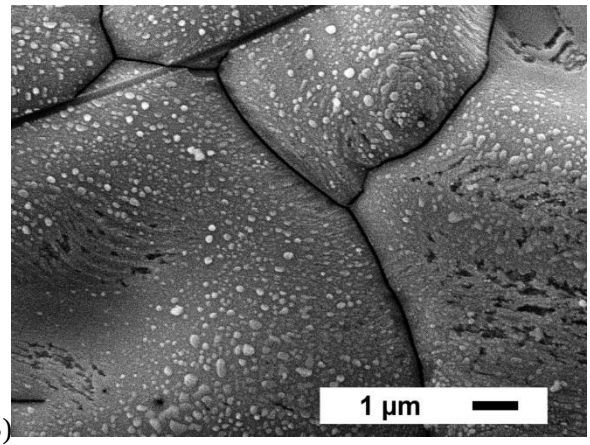

Figure S7. Representative SEM images of the electrode surface obtained during the electrochemical activation of the silver screen-printed electrode in presence of LiClO4. **A)** SEM image when the voltammetric sweep was recorded between +0.5 and +0.35 V (stopped during the oxidation stage) and **B)** SEM image when the voltammetric sweep was recorded between +0.5 and +0.0 V, where the SERS signal was maximum.

The electrode surface is also etched during the oxidation stage in a similar way to the experiment performed in KNO_3 because the silver is oxidised and soluble species are formed. No significant structural differences were visually found compared between both surfaces at these potentials. However, the cyclic voltammetry shows that the oxidation charge is significantly lower in presence of $LiClO_4$ compared to KNO_3. This fact has a significant impact on the structure of the generated particles during the reduction stage. In this case, a higher particle density but with smaller dimensions are found all over the surface as the amount of oxidised silver is lower. The different silver nanostructure seems to be fundamental to explain the different SERS signal in $LiClO_4$ or KNO_3 as the potential where the maximum SERS signal is obtained is very close for both electrolytes. It is also not unreasonable to think that the different adsorption of the electrolyte ions on the silver surface could have some influence on the SERS activity.

Estimation of the approximate number of detected molecules

We tried to estimate the approximate number of molecules that could be covering the silver surface during the SERS detection. The lowest detectable concentration of ferricyanide was $5x10^{-10}$ M, which in different units is $5x10^{-25}$ mol μm^{-3}. Converting this value to number of molecules using Avogadro's number, the lowest detectable concentration was 0.301 molecules μm^{-3}. The volume of solution detectable by SERS is defined by the spot diameter of the laser source, which is around 200 µm, and by the thickness of the solution where the molecules are in contact with the electrode surface. As shown in the main manuscript, the relationship between the concentration and the SERS intensity follows fairly well a Langmuir isotherm, which assumes that the surface is covered at most by a monolayer of the chemical probe. It is reasonable to think that at these ultralow concentrations the surface is not even covered by the complete monolayer. Therefore, the thickness of the detected volume is at most the thickness of a ferricyanide molecule. We performed computational calculations in order to estimate the thickness of a ferricyanide molecule strongly adsorbed on a silver surface. Avogadro software with Universal Force Field (UFF) was employed to optimize the molecular structure adsorbed on the silver surface. **Figure S8** shows the optimized geometry and the distance between the silver atom and the last nitrogen of the molecule, which was 0.823 nm. The estimated SERS detectable volume considering the laser spot diameter and the molecule coverage was 25.85 μm^3. Therefore, the number of molecules estimated in the detectable volume was 7.8 molecules. As mentioned, this is a rough calculation and several factors could influence this value: not all the electrode surface is covered by silver particles (this factor would lower the estimated number of molecules), it is well-known that nanostructures increase the surface area (this factor would increase the estimated number of molecules) and at the lower concentrations the probe molecules are probably in a sub-monolayer coverage (this factor would lower the estimated number of molecules). Therefore, these rough calculations, although approximate, seem to suggest that the detection of ferricyanide is very close to the single-molecule limit.

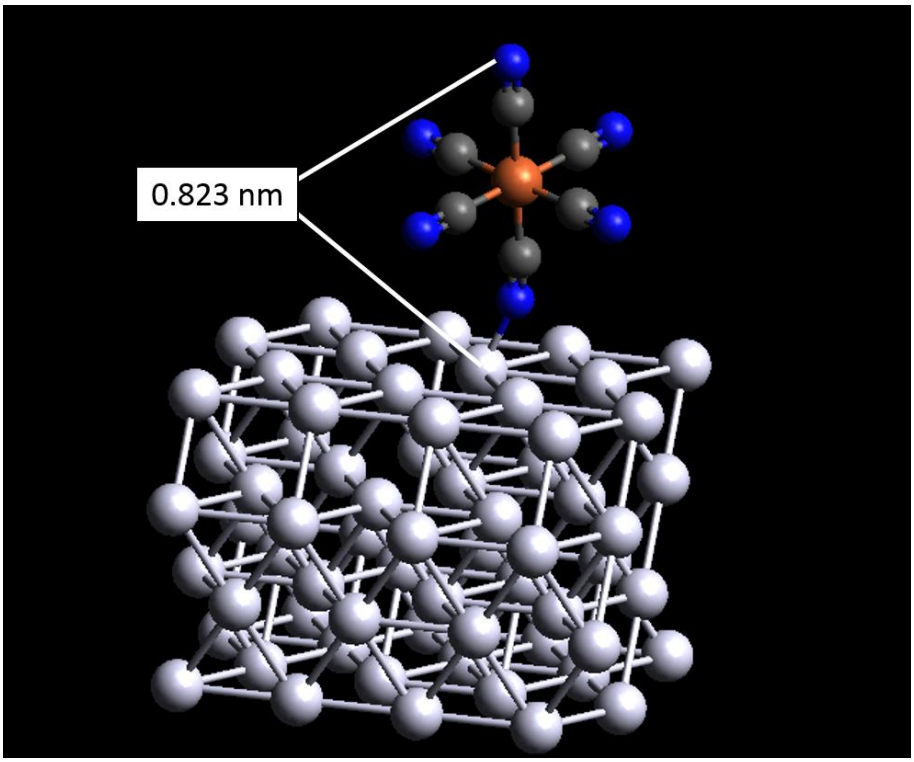

Figure S8. Schematic of the optimized structure of ferricyanide adsorbed on a silver surface illustrating the distance between the first silver atom of the substrate and the last nitrogen atom of the molecule.